Lawrence Berkeley National Laboratory
Recent Work

Title
IMPROVED RESOLUTION METHODS FOR BEAM FOIL SPECTROSCOPY

Permalink
https://escholarship.org/uc/item/19z2q9hw

Authors
Hadeishi, T.
Michel, M.C.
Yellin, J.
et al.

Publication Date
1973-02-01

C·|

IMPROVED RESOLUTION METHODS FOR
BEAM FOIL SPECTROSCOPY

T. Hadeishi, M. C. Michel, J. Yellin and E. Geneux

February 1973

DISCLAIMER

LBL-1260

IMPROVED RESOLUTION METHODS FOR BEAM FOIL SPECTROSCOPY[*]

T. Hadeishi, M. C. Michel, and J. Yellin

Lawrence Berkeley Laboratory
University of California
Berkeley, California 94720

and

E. Geneux

Institut d'Optique Physique
Lausanne, Switzerland

February 1973

Abstract

In general, the resolution that can be achieved by conventional beam foil spectroscopy is limited by the effects of cascading, spread in the beam velocity, beam divergence and uncertainty in the beam velocity. We shall discuss a class of experiments which does not depend on these   properties of the ion beams from low energy accelerators. We believe that by proper choice of experimental conditions, extremely high precision can be achieved by the technique of beam foil spectroscopy.

---

1. Introduction

The most remarkable property of beam foil spectroscopy (BFS), in our opinion, is that the excitation occurs at a well defined time (foil position) in the extremely short time of about 10^{-5} nsec. This property has been used over the past several years to measure mean-lives of excited states of atoms and ions. In the past three years, in collaboration with the beam-foil group at the University of Arizona, we started a program to observe other phenomena such as atomic and ionic alignment with the hope that methods may be found to yield measurements of improved resolution and precision. We believe that the first clue to the possibility of high resolution experiments was the observation that atoms and ions which are excited by the foil are aligned to a sufficiently high degree that experiments based on alignment can be performed[1]. Similar experiments were carried out, in the case of beam-gas collisions by Ray Hughes[2] and a group under Dufay in Lyon[3]. A theory was developed by Van den Bos[4] for the proton-hydrogen collision. In the case of the electron capture process by protons of high velocity from the hydrogen atom, the theory predicts that the cross section for capture leading to states of lower magnetic quantum number is larger than for capture to higher quantum number states. Here, the axis of quantization is along the beam direction. In other words, the theory predicts that the excited states formed by the electron capture process are aligned along the beam direction for high velocity ions. The experimental results of several investigators have shown that the gross features of the experimental observations agree with the theory. Although the excitation process involved in the case of atoms and ions passing through a foil is much more complicated than beam-gas collisions, the atoms and ions are aligned in a manner very

similar to that of gas collisions. In general, excited states of almost all

the atoms and ions formed by beam-foil collisions have been shown to be aligned

for those states that are characterized by $L \geqslant 1$, J and $F > 1/2$. Thus, for

the atoms and ions aligned by beam-foil and beam-gas collisions, the technique

of Hertzian (or R.F.) spectroscopy, first developed by Brossel and Bitter[5]) in

1952, can be applied. The basic advantage of RF spectroscopy over conventional

optical spectroscopy is that the precision of the measurements is not influenced

by Doppler broadening. Thus, most high precision measurements have been made

by a form of RF spectroscopy. About 10 years after the development by Brossel

and Bitter, of RF resonance techniques for excited states of atoms, the non-zero

field Hanle Effect (level crossing) technique was developed by Franken[6]). The

precision of measurements made by the level-crossing technique is also

dependent only on the natural line width and is not affected by Doppler broadening.

Remarkable advances in RF spectroscopy took place soon after. These were;

light beats by Dodd and Series[7]), anti-level crossing by Wieden and Eck[8]), and

many phenomena associated with quantum field theory, developed primarily by Cohen-

Tannondji[9]). None of these phenomena can be observed unless the states are

either aligned or polarized. Conversely, if atoms or ions are aligned, all of

these phenomena are observable, at least in principle.

We have been conducting a systematic study to attempt to apply these

techniques developed by RF spectroscopists to beam foil spectroscopy. However,

we must understand the basic differences between the two methods. One of the most

important is that in the case of RF spectroscopy (including the atomic beam technique),

the atoms move at thermal velocities on the order of 10^5 cm/sec. On the other

hand, in BFS the atoms or ions move at velocities of 10^8 cm/sec or higher.

Thus, we must consider the uncertainty principle relation $\Delta\nu\Delta t \sim 1$. In the case of RF spectroscopy Δt is the life-time of the state while $\Delta t(obs)$ for BFS can vary from a fraction of a life-time to several life-times. In BFS, the precision, $\Delta\nu \sim 1/\Delta t$, can be varied over a considerable range depending on the experimental conditions. Roughly speaking, if one can set the experimental conditions so that $\Delta t(obs) > \tau$ (the mean-life of the state), $\Delta\nu$ can be below the natural line width. Meeting these experimental requirements is an extremely difficult task in RF spectroscopy while relatively simple in BFS. We shall discuss the basic features of experiments that can achieve high resolution by arranging the experimental condition so that $\Delta t(obs) > \tau$.

2. Theory of Improved Resolution by BFS

In general, there are two basic techniques available that should yield high precision measurements; RF resonance and level crossing. By conventional methods, the RF resonance and level crossing phenomena are integrated over a time interval much longer than the mean-lives of the states of interest since atoms involved in the resonance or level crossing remain in the interaction region for a time long compared with the mean-life of the state. Thus, the resonance width is approximately $\Delta V \sim \frac{1}{\pi \tau}$ where τ is the life-time of the excited state.

On the other hand, by BFS, because of the high velocity of the atoms and ions, one can quite readily make an observation at a time longer than the natural life-time. Such a detection method was used by Ma, et al. for an RF resonance experiment[10]) and Copley, Kible, and Series[11] for a level-crossing experiment. Both of these experiments were carried out using a conventional light source (not BFS source). We believe that the technique developed by these investigators is most suitable for BFS.

The experimental condition we are interested in is one in which an ion beam passes through a thin foil resulting in the alignment of excited states of ion or atom. Now, let the beam interact with an oscillating RF field or an appropriate level crossing field, and start the detection at a finite time (t) after excitation for a duration Δt.

We shall first describe the time-delayed detection of level-crossing of ^{4}He in the $3^3P_{1,2}$ state for $\Delta M_J = 2$ crossing as shown in fig. 1.

3. Theory

The intensity of light emitted by a ^{4}He atom in the ^{3}P state at time t after excitation and with polarization vector in the y-z plane is given by

$$I(\omega,t) = Ae^{-\gamma t} \{1 + a_1 \cos \omega_{12} t + a_2 \cos \omega_{02} t$$

$$+ a_3 \cos(2\omega t + 2\theta) + a_4 \cos[(\omega_{12} - 2\omega)t - 2\theta]$$

$$+ a_5 \cos[(\omega_{12} + 2\omega)t + 2\theta] + a_6 \cos[(\omega_{02} - 2\omega)t - 2\theta]$$

$$+ a_7 \cos[(\omega_{02} + 2\omega)t + 2\theta]\}$$

and the signal observed by a detector with a slit extending from ℓ_1 to ℓ_2, is given by $S(\omega) = \int_{t_1}^{t_2} I(\omega,t)dt$, where ω_{ij} are the fine structure separations, $\omega = g_J \mu_0 H/t$ and θ is the angle which the electric field vector of the light makes with the beam axis as in fig. 2. The coefficients a_i are determined by the initial state and angular factors from the electric dipole matrix element; t_1 and t_2 are defined by $t_1 = \ell_1/v$, $t_2 = \ell_2/v$ where v is the beam velocity.

The atom is assumed to emerge from the foil in an aligned state $\psi = |L = 1\ m_L = 0, S = 1\ m_s\rangle$ with respect to the beam direction. In the presence of a magnetic field H along the z-axis the state vectors are rotated by $\pi/2$ so that expanding ψ in Jm states we may write

$$\psi(t = 0) = \sum_J \sum_{m_J'} C_{m_J}^{(0)} \mathcal{D}_{m_J',m_J}^{(J)} (0,\pi/2,0)$$

The time evolution of ψ is obtained by solving the Schrodinger equation for the coefficients C(t) from which the intensity fluctuations are derived.

The above result is strictly true only for low magnetic fields where $\omega \ll \omega_{ij}$. In the region of our interest $2\omega \sim \omega_{1,2}$. Here the eigenfunctions are no longer those of J_z. The Zeeman interaction mixes the m_J states and the solution of the Schrodinger equation is very much complicated and must be carried out numerically. If we confine our attention to the region of the two crossings $(2,0)$ and $(1,-1)$ then the signal observed by a detector having a finite slit width can be represented by two terms

$$S(\omega) = \int_{t_1}^{t_2} Be^{-\gamma t} \cos[(\omega' - 2\omega)t - 2\theta]dt$$

$$+ \int_{t_1}^{t_2} Ce^{-\gamma t} \cos[(\omega'' - 2\omega)t - 2\theta]dt$$

where $\omega = (\frac{\partial w}{\partial H})/\hbar$ where w is the energy, t_1 is the time at which observation begins (ℓ_1/v), and t_2 the time at which observation ends (ℓ_2/v). The high frequency components integrate out rapidly and contribute very little to the signal. The constant part of the signal is dropped for simplicity. Figure 1 shows the level crossings in the $^3P_{1,2}$ states of ^{4}He. The integrations are readily performed and in figs. 3-5 the signal is shown as a function of the parameters t_1, t_2, θ, and H. In these calculations we have taken $B = C$ and justify this for the present on experimental grounds. Our purpose here is not to fit line shapes but to show in a quantitative way how the signal behaves with the various parameters available to us in beam foil work. By proper selection of t_1 and t_2, the two crossings, at 161.7 and 166.5 gauss can be picked out with high accuracy as illustrated in fig. 6. Although the modulation in the wings is an appreciable fraction of the

crossing signal they can be distinguished from the crossings by shifting the limits of

integration (i.e., shifting the detector aperture up or down stream). In that

case the position (and frequency) of the modulation changes but the level

crossing peaks do not move.

The expression for RF resonance can be obtained by a similar calculation.

The result of the calculation is similar to that for level crossing, again with

undulations in the resonance curve.

4. Experiment

Since alignment is quite an important part of the experiment, we shall
begin our discussion with the data on alignment. Our first experimental result
was that which we performed about two years ago on ^{7}Li alignment by beam foil
and beam-gas electron capture. In the case of foil excitation, we simply
observed quantum beats in the field region given by

$$I(H) \propto e^{-\Gamma t} \left[1 + A \cos \frac{2g_J \beta H}{\hbar} t \right] \quad .$$

Thus, it is evident that one should observe periodic changes in light intensity
as we vary the magnetic field H, keeping t constant by observing at a fixed
distance ℓ down stream from the foil (since $t = \frac{\ell}{v}$).

Figure 2 shows the experimental arrangement and fig. 7 shows typical
experimental results on quantum beats[12]. The polarization ratio
$\pi = (I_\parallel - I_\perp)/(I_\parallel + I_\perp)$ is approximately 5 to 10% at energies of 20 keV to
70 keV, with alignment increasing with energy. In the case of beam gas
collision, the alignment was observed by the Hanle effect[13] (see fig. 8). In
this case, the alignment was 22% which represents complete alignment after
taking the hyperfine interaction into account.

After a few experiments on other atoms by the Arizona group, we came
to the conclusion that the alignment that takes place by BFS approximately
satisfies the proton-hydrogen collision theory, i.e., the cross section for
charge capture in $m_\ell = 0$ state is larger than for $m_\ell > 0$. We have, for the
time being, abandoned the experimental study to determine the mechanism for
alignment and instead have begun a program to achieve high resolution. The

technique we are currently using is level-crossing since we have not yet

constructed an RF field system for resonance work.

We shall compare BFS results with extreme high precision work done by

electron impact excitation at LBL by Dr. Edmond Geneux when he visited our

laboratory. His results are shown in fig. 9. Figure 10 shows the experimental

arrangement for delayed detection of level crossings in ^{4}He and in fig. 11

we give the results of the first successful experiments. The line widths

are still greater than the natural width, but will decrease with increasing

integration. Note the undulations as predicted by the theory.

5. Conclusion

We believe that our experimental observations of time delayed level crossing on ^{4}He show conclusively the powerful feature of BFS for high precision measurements. In addition to the narrow signal width, an additional advantage of BFS is that the experiment is carried out in a vacuum so that the collision effect from the surrounding atoms that usually takes place in conventional rf spectroscopy is absent, and high field stark effect experiments can also be achieved without the problem of electrical breakdown of gas.

FOOTNOTES AND REFERENCES

1) C. H. Liu, S. Bashkin, W. S. Bichel, and T. Hadeishi, Phys. Rev. Letters 26 (1971) 222; T. Hadeishi, R. D. McLaughlin, and M. Michel, J. Opt. Soc. Am. 61 (1971) 653; T. Hadeishi, R. D. McLaughlin, and M. C. Michel, Lawrence Radiation Laboratory Annual Report UCRL-20426, p. 188 (1970)

2) R. H. Hughes, in Beam Foil Spectroscopy (ed. S. Bashkin: Gordon & Breach, Inc., New York, 1968) p. 104

3) M. Carré, J. Desesquelles, and M. Dufay, Phys. Rev. Letters 27 (1971) 1407

4) J. Van den Bos and F. J. DeHeer, Physica 34 (1967) 338

5) J. Brossel and F. Bitter, Phys. Rev. 86 (1952) 308

6) P. A. Franken, Phys. Rev. 121 (1961) 508

7) J. N. Dodd and G. W. Series, Proc. Roy. Soc. (London) A 273 (1963) 41

8) H. Wieden and T. G. Eck, Phys. Rev. 153 (1967) 103

9) C. Cohen-Tannoudji, Thesis, Ann. Phys. 7 (1962) 423

10) I. J. Ma, G. zu Putlitz, and G. Schütte, Physica 33 (1965) 282; I. J. Ma, J. Mertens, G. zu Putlitz, and G. Schütte, Z. Phys. 208 (1968) 352

11) G. Copley, B. P. Kibble, and G. W. Series, J. Phys. B (Proc. Phys. Soc.) Ser. 2, Vol. 1 (1968) 724

12) T. Hadeishi, R. D. McLaughlin, and M. C. Michel, Lawrence Radiation Laboratory Annual Report UCRL-20426, p. 188 (1970); T. Hadeishi, R. D. McLaughlin, and M. Michel, J. Opt. Soc. Am. 61 (1971) 653

13) T. Hadeishi, et al., loc. cit.

FIGURE CAPTIONS

Fig. 1. Level system for ^{4}He, $^3P_{1,2}$.

Fig. 2. Experimental arrangement for BFS measurements involving alignment

by foil or gas collisions.

Fig. 3. Calculated level crossing signal for the ^{4}He, $^3P_{1,2}$ system, polarization

angle of observation = 0°

a) delayed 0.1 τ, integrated over 0.3 τ

b) delayed 0.1 τ, integrated over 0.4 τ.

Fig. 4. Calculated level crossing signal for the ^{4}He $^3P_{1,2}$ system. Polarization

angle of observation = 45° (dispersion signal)

a) delayed 0.1 τ, integrated over 0.3 τ

b) delayed 0.1 τ, integrated over 0.4 τ.

Fig. 5. Calculated level crossing signal for the ^{4}He, $^3P_{1,2}$ system. No delay,

integrated over 10 τ (approximately the natural line-width)

a) polarization observation angle = 0°

b) polarization observation angle = 45° (dispersion signal)

Fig. 6. Calculated level crossing signal for the ^{4}He, $^3P_{1,2}$ system. Delayed

for 1.0 τ, integrated for 2τ. Note line width is below natural width, but

signals are accompanied by undulations resulting from incomplete integration.

Fig. 7. Light beats in ^{7}Li ^2P system for different values L of the distance

from the foil.

Fig. 8. Hanle effect in ^{7}Li, ^2P, observed by beam-foil excitation and alignment.

Fig. 9. Electron impact level crossing in ^{4}He, $^3P_{1,2}$. Data of E. Geneux.

(a) Lower field crossing, (b) Higher field crossing.

Fig. 10. Experimental arrangement for ^{4}He level crossing measurements.

Fig. 11. Observed level crossings in ^{4}He, $3^3P_{1,2}$.

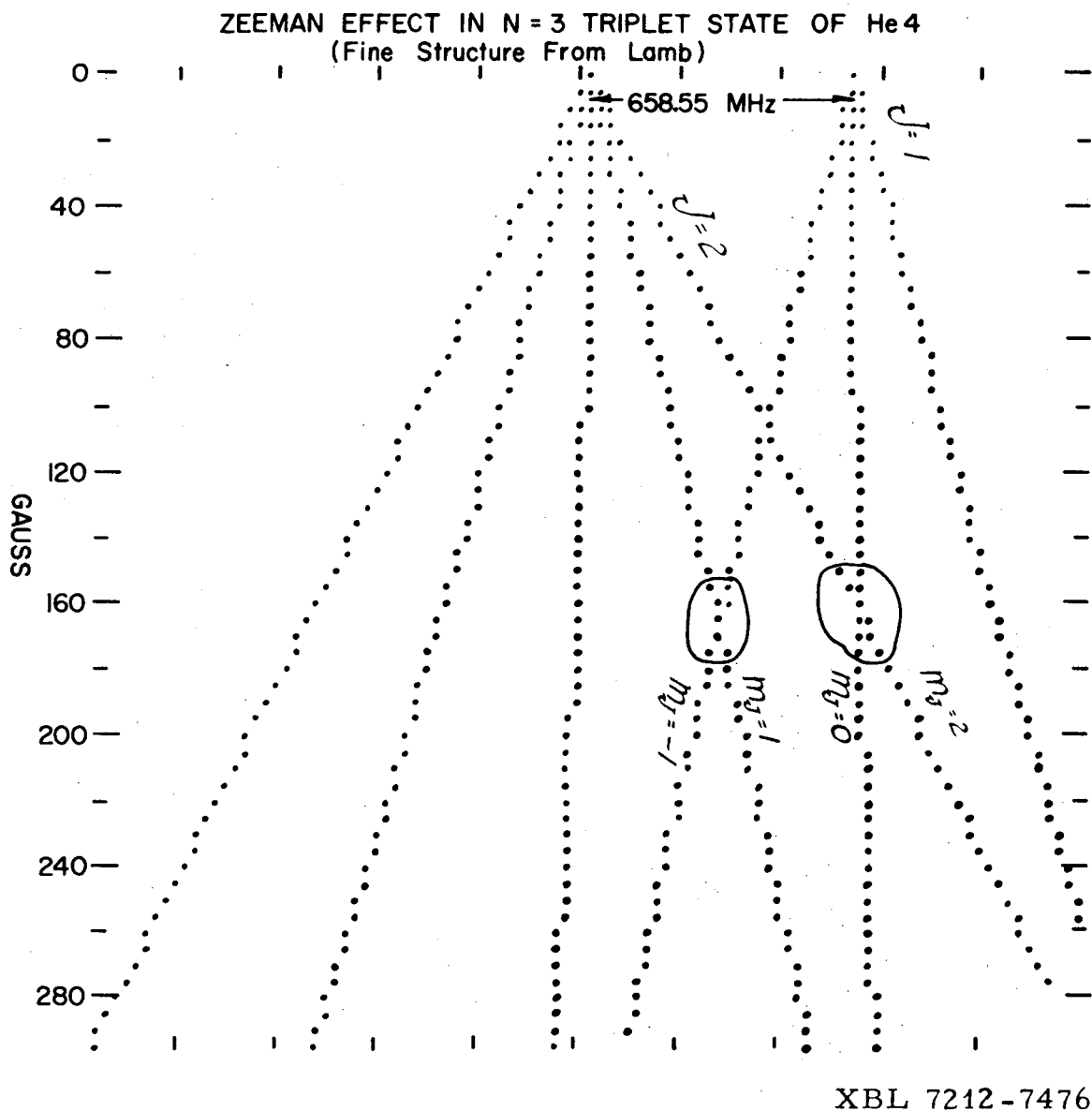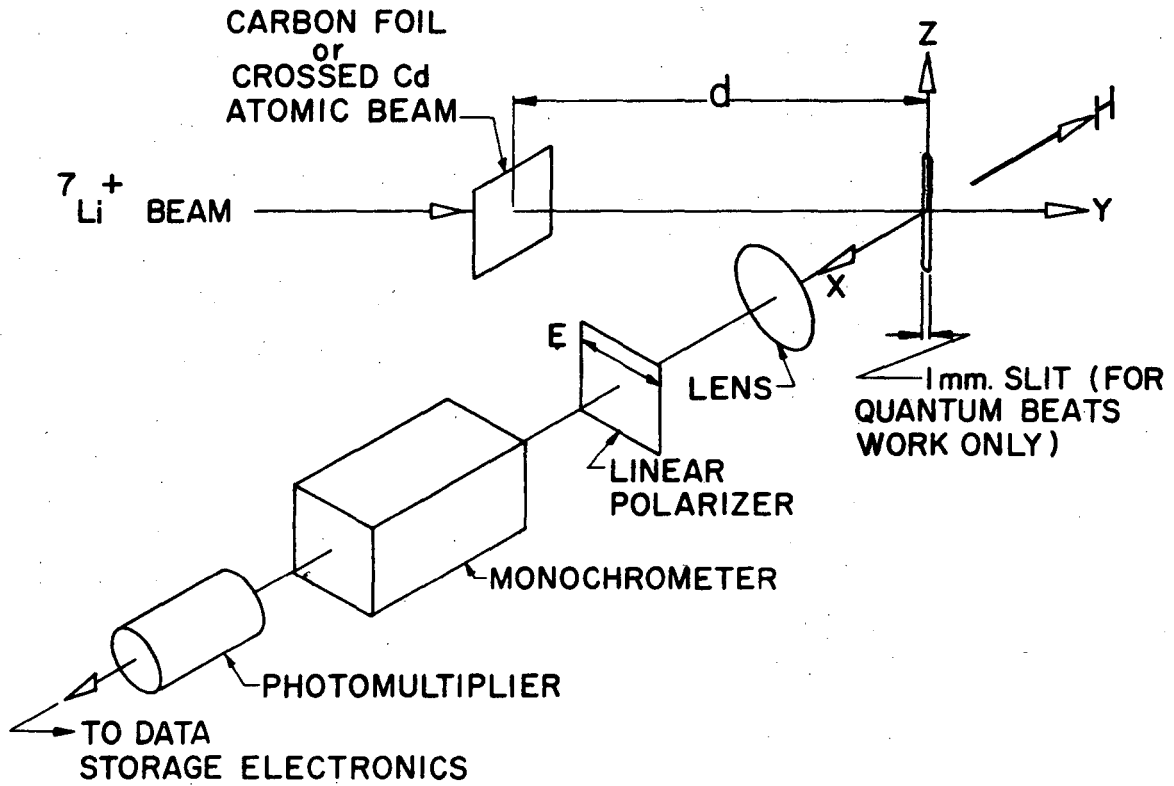ZEEMAN EFFECT IN N = 3 TRIPLET STATE OF He 4
(Fine Structure From Lamb)

XBL 7212-7476

Fig. 1

CARBON FOIL
or
CROSSED Cd
ATOMIC BEAM

$^7_{}Li^+$ BEAM

d

Z

H

Y

X

1mm. SLIT (FOR
QUANTUM BEATS
WORK ONLY)

E

LENS

LINEAR
POLARIZER

MONOCHROMETER

PHOTOMULTIPLIER

TO DATA
STORAGE ELECTRONICS

XBL 713-550

Fig. 2

LBL-1260

144.20— -0.060   RELATIVE SIGNAL
-0.026   0.008   0.042   0.076
148.20—

152.20—

156.20—

GAUSS 160.20—

164.20—   Fig. 3a

168.20—

172.20—   Lifetime = 93.00nSec
                     Gamma T_1 = 0.10, Gamma T_2 = 0.30
176.20—   Observation Angle = 0°

180.20—

144.20— -0.096   RELATIVE SIGNAL
-0.056   -0.017   0.022   0.062
148.20—

152.20—

156.20—

GAUSS 160.20—

164.20—

168.20—   Fig. 3b

172.20—

176.20— Lifetime = 93.00 nSec
         Gamma T_1 = 0.10, Gamma T_2 = 0.40
180.20— Observation Angle = 0°

XBL 7212-7473

Fig. 4a

RELATIVE SIGNAL

144.20 — -0.071   -0.035   0.00   0.036   0.072

148.20 —

152.20 —

156.20 —

GAUSS 160.20 —

164.20 —

168.20 —

172.20 — Lifetime = 93.00 nSec
        Gamma T1 = 0.10, Gamma T2 = 0.30
176.20 — Observation Angle = 45°

180.20 —

Fig. 4b

RELATIVE SIGNAL

144.20 — -0.103   -0.052   -0.001   0.050   0.101

148.20 —

152.20 —

156.20 —

GAUSS 160.20 —

164.20 —

168.20 —

172.20 — Lifetime = 93.00 nSec
        Gamma T1 = 0.10, Gamma T2 = 0.40
176.20 — Observation Angle = 45°

180.20 —

XBL 7212-7474

RELATIVE SIGNAL

Fig. 5a

Lifetime = 93.00 nSec.
Gamma T₁ = 0 , Gamma T₂ = 10.00
Observation Angle = 0°

RELATIVE SIGNAL

Fig. 5b

Lifetime = 93.00 nSec
Gamma T₁ = 0 , Gamma T₂ = 10.00
Observation Angle = 45°

XBL 7212-7475

XBL 729-1884

Fig. 6

LBL-1260

Fig. 7

XBL 713-549

Fig. 8

XBL 713-547

Fig. 9a

XBL 729-1918

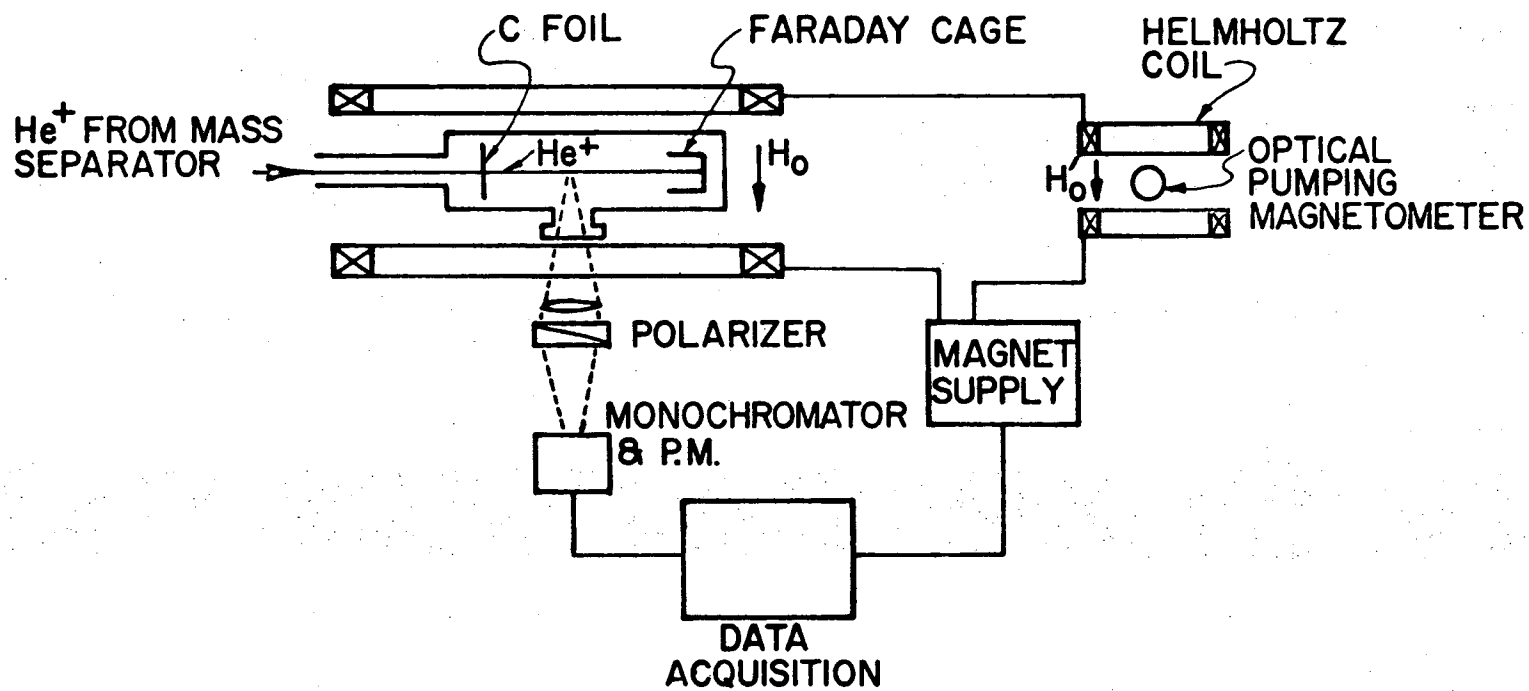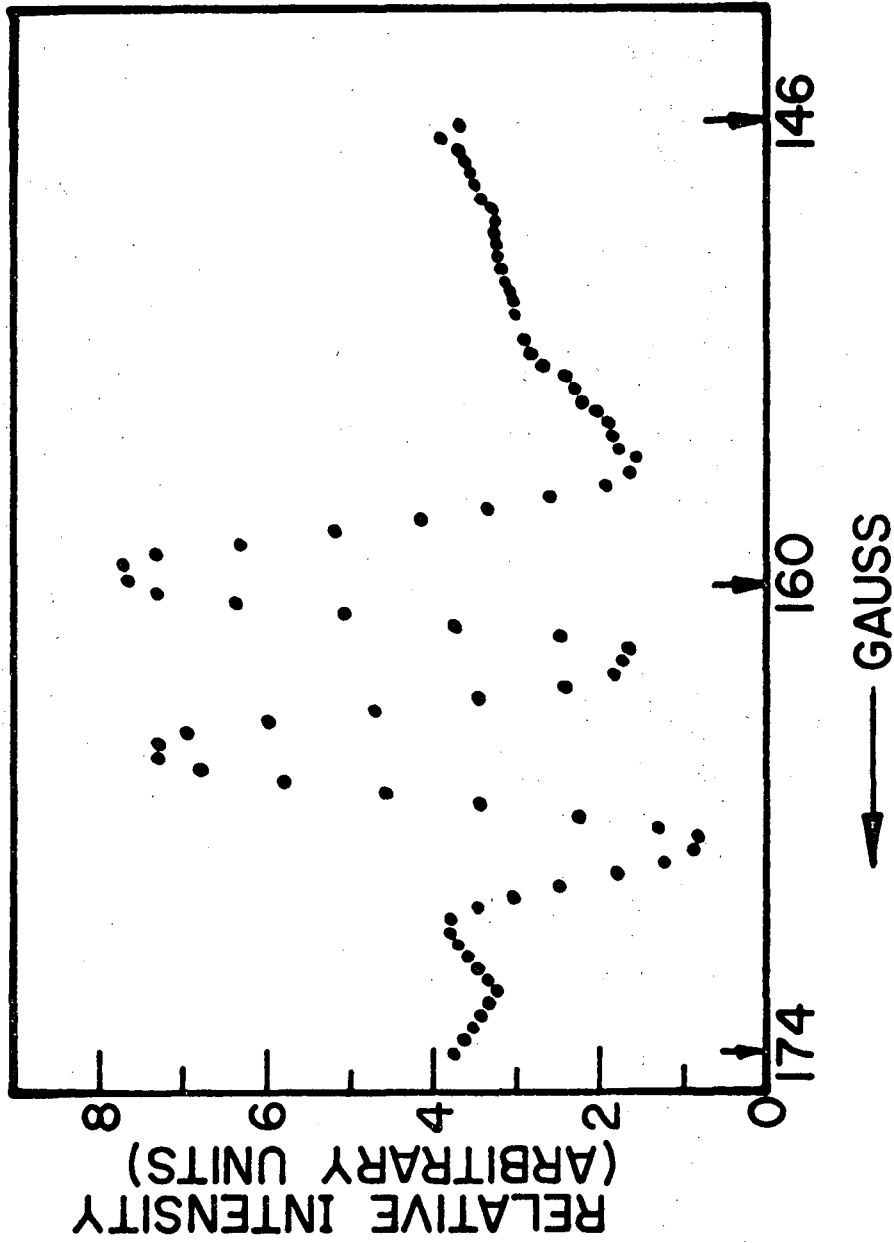LBL-1260

XBL 729-1919

Fig. 10

XBL 729-1917

XBL 729-1949

Fig. 11